A framework for Active Contour initialization with application to liver segmentation in MRI*

A. Mir-Fuentes[1,2][0000−0001−5914−9860], A. Mir[4,5][0000−0001−5282−3699], F. Antunes-Santos[1,2,3][0000−0003−3298−9215], F.J. Fernandez[1][0000−0003−4427−3935], and C. Lopez-Molina[1,2,3][0000−0002−0904−9834]

[1] Dept. of Estadística, Informática y Matemáticas, Universidad Pública de Navarra
31006 Pamplona, Spain
E-mail: {arnau.mir, felipe.antunes, fcojavier.fernandez, carlos.lopez}@unavarra.es

[2] NavarraBiomed, Hospital Universitario de Navarra
31008 Pamplona, Spain

[3] KERMIT, Dept. of Data Analysis and Mathematical Modelling, Ghent University,
9000 Ghent, Belgium;

[4] Department of Mathematics and Computer Science, Univ. of the Balearic Islands
07122 Palma, Spain
E-mail: arnau.mir@uib.es

[5] Health Research Institute of the Balearic Islands (IdISBa),
07010 Palma, Spain

Abstract. Object segmentation is a prominent low-level task in image processing and computer vision. A technique of special relevance within segmentation algorithms is active contour modeling. An active contour is a closed contour on an image which can be evolved to progressively fit the silhouette of certain area or object. Active contours shall be initialized as a closed contour at some position of the image, further evolving to precisely fit to the silhouette of the object of interest. While the evolution of the contour has been deeply studied in literature [11, 5], the study of strategies to define the initial location of the contour is rather absent from it. Typically, such contour is created as a small closed curve around an inner position in the object. However, literature contains no general-purpose algorithms to determine those inner positions, or to quantify their fitness. In fact, such points are frequently set manually by human experts, hence turning the segmentation process into a semi-supervised one. In this work, we present a method to find inner points in relevant object using spatial-tonal fuzzy clustering. Our proposal intends to detect dominant clusters of bright pixels, which are further used to identify candidate points or regions around which active contours can be initialized.

Keywords: Hepatic steatosis · Image segmentation · MRI image · Active Contour Model · Spatial fuzzy c-means · Connected component · Center.

* The authors gratefully acknowledge the financial support of the grants PID2019-108392GB-I00 funded by MCIN/AEI/10.13039/501100011033, as well as that by the Government of Navarra (PC082-083-084 EHGNA). A. Mir acknowledges the financial support of the grant PID2020-113870GB-I00 funded by MCIN/AEI/10.13039/501100011033/.

1 Introduction

Hepatic steatosis is a common condition caused by the storage of residual fat in the liver. In some cases hepatic steatosis can rapidly lead to liver damage, but early detection and control of the disease can often prevent or even reverse hepatic steatosis with lifestyle changes. While detection can be done with invasive procedures, the ideal case is using non-invasive methods, which are safer, faster and, thanks to the innovations in medical imaging, significantly more accurate. Among non-invasive methods, medical imaging offers a wide range of alternatives with application to the task. Liver segmentation can be achieved with a range of strategies, from thresholding algorithms to neural networks [13, 14]. Within such range of alternatives, active contours appear as a prominent one. Active contour models (ACMs), also called snakes, are deformable curves that evolve according to predefined forces. Such forces are normally designed to pull the curve in the normal direction, seeking to minimize an energy functional defined over the space where the curves are defined. Active contour models may be understood as a special case of the general technique of matching a deformable model to an image by means of energy minimization in two dimensions. In this work, ACMs [10] have been chosen over other alternatives for liver segmentation because they do not require training data, they are unsupervised, they have fast convergence and, also, they are robust to noise and topological changes. Interestingly, ACMs allow to control the regularity of objects and their contours adapting the resulting spline to the expected characteristics of the object.

Active contour models were initially introduced by Kass *et al.* in 1988 [10], as part of an effort to apply deformable models in image processing [20]. Among the different follow-up works, the one by Caselles *et al.* [4] is of special relevance. In [4], the authors did not only improve ACMs by giving a more consistent equation for the energy functional, but also gave some proofs on the convergence and stability of ACMs considering viscosity solutions [8]. Despite relevant advances in ACMs, their development has been an ongoing research effort over the past decades. For example, [12] improved the definition of the energy functional equation by adding terms that improve the regularity and speed of convergence.

One of the recurrent problems in the practical use of ACMs is the need to define an initial contour, which is often done manually. In this work, we present different strategies to find a suitable initial curve for ACMs. Note that this task does not only restrict to finding any inner position in a generally-defined object. Also, the selection of the contour shall attempt the point (or the initial contour around it) to have optimal performance for ACMs in terms of convergence and accuracy. The problem we aim at can be stated as follows: Given a grayscale image containing an object of interest, find an initial curve within that object to be used as initial contour in an ACM. The object to be found verifies a local fuzzy property, which is key for our algorithm. In our case, the grayscale image is the MRI visualization of a human torso, the object to be found is the liver and the local fuzzy property is the amount of water at each position. The use of MRI is due to the fact that it comprises a direct relationship between the amount of water and the gray level intensity at each position of the image.

The remainder of this works is divided as follows. In Section 2 we present a general framework for ACM initialization, which is instantiated in Section 3. Our proposal is put to the test in Section 4, while Section 5 lists some conclusions.

2 A framework for Active Contour Model initialization

In this work, images are taken as mappings $\Omega \mapsto \mathbb{T}$, with Ω representing the set of positions in the image grid and $\mathbb{T}$ represents the tonal palette. The term $\mathbb{I}_{\mathbb{T}}$ represents the set of images with a certain tonal palette $\mathbb{T}$. For example, $\mathbb{I}_{\{0,1\}}$ represents the set of binary images, while $\mathbb{I}_{[0,1]}$ is the set of real-valued grayscale images. More complex instantiations of $\mathbb{T}$ could be, for example, hyperspectral signatures [15].

Definition 1 (Inclusion of binary images). *Given two binary images I and J, image I is included in image J, $I \subseteq J$, when $I(x,y) \leq J(x,y)$, $\forall (x,y) \in \Omega$.*

Definition 2 (Inclusion of binary and grayscale images). *Given $t \in (0,1)$ a threshold, I a binary image and J a grayscale image, image I is included in image J using threshold t, $I \subseteq_t J$, when $I(x,y) \leq J_t(x,y)$, $\forall (x,y) \in \Omega$, where J_t is the "binarized" J image defined as:* $J_t(x,y) = \begin{cases} 1, & \text{if } J(x,y) \geq t, \\ 0, & \text{otherwise.} \end{cases}$

We propose a novel framework to find the most appropriate center (pixel) around which the initial curve of an ACM can be located. Inspired by the developments of Bezdek *et al.* on edge detection [2], our proposal is based on a four-step procedure in which each phase takes an interpretable goal. The four phases in our proposal are:

- *Object detection*: This is the phase in which visual information is processed to produce an initial estimation of the presence of the object of interest. It is expressed as a mapping $f_{OD} : \mathbb{I}_{\mathbb{T}} \mapsto \mathbb{I}_{[0,1]}$ which intends to locate the areas of the image in which the object is present. There is no constraints in the tonal palette of the input image (which might be dependent upon specific scenarios), but the output needs to be a value in $[0,1]$. This value is not interpreted as a probability, but as a fuzzy membership degree representing the certainty on the membership of the pixel to the object of interest.
- *Object Selection*: This phase consists of selecting the contiguous area containing the object of interest, out of the information produced at the object detection phase. It can be modeled as a mapping $f_{OS} : \mathbb{I}_{[0,1]} \mapsto \mathbb{I}_{\{0,1\}}$, so that (a) the set of 1-labeled pixels in $f_{OS}(I)$ form a connected component and (b) $f_{OS}(I) \subseteq_t I$, where t is the threshold from which the pixels belong to the region where the object can be. This represents the fact that (a) one singular object is selected and (b) the object selection phase aims at selecting one the areas identified at the previous phase, not modifying the representation of such area.

- *Object Isolation*: This is the phase in which the morphological priors of the object of interest need to be enforced. Object detection and segmentation in real applications is heavily affected by a list of accepted priors, which can impose restrictions on the object, including shape, regularity, position, etc. The object isolation phase is expressed as a mapping $f_{OI} : \mathbb{I}_{\{0,1\}} \mapsto \mathbb{I}_{\{0,1\}}$ in which the only restrictions to the output are driven by the context of application.
  Note that this phase does not intend to produce a faithfull (or reliable) segmentation of the object. It rather intends to make an approximate detection, in which exactitude shall not be requested. However, regardless of how good the approximation is, we understand that some priors can and should be enforced. For example, an approximate segmentation of a liver might contain lack of precision in the boundaries, but should not contain holes or 1-pixel width linear structures, which are biologically non-viable.
- *Center selection*: This is the phase in which the approximate segmentation is analyzed in order to look for a center around which an initial contour can be set. This can be done on the basis of different inspirations, and is represented as a mapping $f_{CS} : \mathbb{I}_{\{0,1\}} \mapsto \Omega$, with $I(f_{CS}(I)) = 1$ for any binary image I.

Our proposal is divided in four phases which can be combined by function composition. Otherwise said, center detection can be expressed as a function $f_{CD} : \mathbb{I}_{\mathbb{T}} \mapsto \Omega$, which can be broken down as

$$f_{CD}(I) = f_{CS}(f_{OI}(f_{OS}(f_{OD}(I)))) \ . \tag{1}$$

The following section includes a specific implementation of the proposed framework with application to liver segmentation in MRI imagery.

3 Active Contour Model initialization for liver segmentation in MRI imagery

In this section we present a specific implementation of the framework in Section 2. Specifically, we present an implementation aimed at initializing ACM models for liver segmentation in MRI imagery. This application is relatively frequent in public health and nutrition studies, in which non-invasive liver analysis is a recurrent diagnosis procedure. In this context, layered images from the MRI are analyzed to both (a) quantify the topological characteristics of the liver and (b) measure visual evidence from its state. The workflow for ACM initialization in such context is as presented in Figure 1.

3.1 Spatial fuzzy *c*-means for Object Detection

Object detection is the phase in which the relevant object has to be discriminated from the remainder of the image. This discrimination need not be precise in any aspect, rather presenting a rough discrimination of the object. Starting a segmentation (ACM) algorithm with a rough approximation to the solution

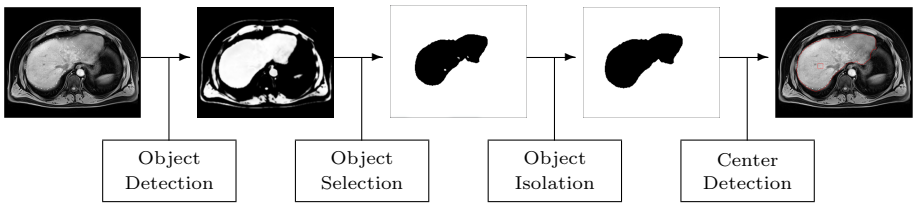

Fig. 1. Schematic representation of the framework presented in Section 2, applied to the problem of ACM initialization for liver segmentation. The original image is presented as a colorized image to improve visibility.

might seem noticeable but is rather common in literature. For example, any context-aware smoothing algorithm (as Anisotropic Diffusion [18, 21]) perform an estimation of the presence and strength of object boundaries before modelling tonal diffusion at each iteration. In this case, the estimation shall be good enough to extract the object from the background.

There is little technical requisites to the object detection phase. In fact, simplistic approaches to the task can be made using fuzzy thresholding, which would discriminate bright areas from dark ones according to their tone. The selection of the thresholding algorithm is dependent upon the characteristics of the image. Classical binary thresholding algorithms would provide binary representations of the object. For example, the Otsu method [17] is designed for images with bimodal histograms, while the Rosin method [19] would rather discriminate outliers in a monomodal histogram. However, this approach is not recommended, since it collides with the spirit of the Object Detection phase. Using fuzzy thresholding algorithms [3] does provide a solution to this, since these algorithms typically produce membership information each pixel other than 0 or 1 values for each class. Otherwise said, fuzzy thresholding does not only lead to the discrimination of the pixels in the image, but also to the gradual quantification of such discrimination. A better suited alternative for object detection is, in this regard, clustering algorithms.

The use of clustering algorithms in image binarization lies on a simplistic interpretation: each pixel in the image can be taken as an instance in a dataset [6, 16]. Such instance would be composed of the spatial information (pixel location) the tonal information and, potentially, other derived information (texture indicators, etc.). The separation of the instances in such dataset, by means of a clustering algorithm, would be able to group together pixels which are both spatially and tonally close. We believe this ability is crucial in selecting clustering algorithms over thresholding algorithms for object detection.

A clustering algorithm able to account for accounting for spatio-tonal information is the Spatial Fuzzy c-Means algorithm (SFCM), which accommodates the use of different metrics within the framework of the well-studied FCM [1]. The SFCM has been selected over other clustering algorithms because it combines the flexibility of the metric adjustment with two important characteristics:

(a) ability to represent the centroids and (b) fuzzy representation of the membership to the classes.

Let $X = \{\mathbf{x}_1, \mathbf{x}_2, \ldots, \mathbf{x}_n\}$ be a set of points over a $k+1$-dimensional Euclidean space $\mathbb{E}$ and $U = \{\mu_1, \ldots, \mu_c\}$ a set of membership functions defined over $\mathbb{E}$. That is, each μ_j is a function:

$$\mu_j : \mathbb{E} \longrightarrow [0, 1] \ ,$$

such that:

$$\sum_{j=1}^{c} \mu_j(x) = 1$$

where, given $\mathbf{x} \in \mathbb{E}$, $\mu_j(\mathbf{x})$ represents the membership degree of point $\mathbf{x}$ to cluster C_j.

The goal of the FCM [1] is to minimize the goal function given by:

$$\sum_{j=1}^{c} \sum_{i=1}^{n} \mu_j(x_i)^m \left\| \mathbf{x}_i - \mathbf{v}_j \right\|^2 , \tag{2}$$

where $m > 1$ is a parameter of the algorithm that controls the importance between the distance and the membership function, $\| \cdot \|$ is the Manhattan, Euclidean or Chebyschev norm. $\mathbf{v}_j$, $j \in \{1, \ldots, c\}$ are the centers of the c clusters, considering the membership function. Such centers are computed as

$$\mathbf{v}_j = \frac{\sum_{\mathbf{x}_i \in C_j} \mu_j(\mathbf{x}_i)\mathbf{x}_i}{\sum_{\mathbf{x}_i \in C_j} \mu_j(\mathbf{x}_i)}, \tag{3}$$

where C_j represents the cluster j,

Given m and the set X, the schema of the algorithm is as follows:

(1) *Initialization*: choose the membership of all the points of set X randomly. For every $\mathbf{x}_i \in X$, $i = 1, \ldots, n$, compute $j = \max_{k=1,\ldots,c} \mu_k(\mathbf{x}_i)$. Next, add the point $\mathbf{x}_i$ to the cluster C_j. In this way, we have calculated the clusters $C_1, \ldots, C_c$. Set the number of iterations n to 1: $n = 1$.

(2) *Computation of the centers*: compute the centers of the algorithm using expression (3). Compute the objective function using expression (2). Let O_i be this value.

(3) *Update of the membership function:* Update the membership function of each point $\mathbf{x}_i \in X$ using this expression:

$$\mu_j(\mathbf{x}_i) = \frac{1}{\left(\sum_{k=1}^{c} \frac{\|\mathbf{x}_i - \mathbf{v}_j\|}{\|\mathbf{x}_i - \mathbf{v}_k\|} \right)^{\frac{2}{m-1}}}, \tag{4}$$

for $i \in \{1, \ldots, n\}$ and $j \in \{1, \ldots, c\}$. Compute the new clusters using the procedure of the first step. Compute the new value of the objective function using expression (2). Let O_{i+1} be this value. Increase the number of iterations n.

(4) *Stopping criterion:* If $|O_i - O_{i+1}| < \epsilon$, where ϵ is the allowed tolerance or if $n \geq n_{\max}$, where $n_{\max}$ is the maximum number of iterations, we stop the process. Otherwise, we go to the step (2) and continue.

While the FCM algorithm has proven valid in a list of applications, we introduce the spatial fuzzy c-means (SFCM) algorithm, which is a generalization of the former. This generalization allows for a better modelling of the distance between elements in the set.

The SFCM is an extension of FCM in which step (3) has two substeps:

(3.1) Update the membership function of each point $\mathbf{x}_i \in X$ using expression (4).

(3.2) Re-update the membership function of each point $\mathbf{x}_i \in X$ using this expression:

$$\mu'_j(\mathbf{x}_i) = \frac{\mu_j(\mathbf{x}_i)^p h_{i,j}^q}{\sum_{k=1}^{c} \mu_j(\mathbf{x}_i)^p h_{i,j}^q},$$

where p and q are parameters that controls the relative importance of the neighbor pixels and $h_{i,j}$ is computed as:

$$h_{i,j} = \sum_{x_j \in NB(x_j)} \mu_i(\mathbf{x}_j),$$

where $NB(\mathbf{x})$ is the set of pixels that belong to the 9×9 square centered at point $\mathbf{x}$. Notice that for $p = 1$ and $q = 0$ the algorithm is exactly the fuzzy c-means algorithm. That is why the spatial fuzzy c-means algorithm are a generalization of the fuzzy c-means algorithm.

It is hence evident why the spatial fuzzy c-means algorithm takes into account the spatial information of the pixels in the substep (3.2).

3.2 Object selection

Object detection is meant to identify the areas of the image which fit to the expected characteristics of the object of interest. However, it might be the case where more than one region or object is selected. The Object Selection phase shall analyze the image and select the isolated region which is more prone to be the object of interest. The selection of the object might also involve certain restrictions in the size of the object, its shape or proportions, its location or even the roughness of its boundaries.

In the case of liver segmentation, our constraints stem from the basics of MRI technology. In MRI visualization, the regions of a body with greater water indices appear brighter than those with lower water indices. We intend to capitalize on this information to produce an object selection procedure. In this application, we opt out by selecting the largest cluster as region of interest. This idea is based on the fact that the cluster representing the background is larger than the cluster representing the object.

For the experimental results, we restricted to the last strategy. This decision is, still, dependent upon the specific imagery.

3.3 Object isolation

Once the image has been discriminated into the *object region* and the *background region*, the next step is to find best fitting area among those labeled as *object region*. In our case, we have opted out by selecting the largest connected component of the cluster that contains the object.

To find the largest connected component, we visualize the binary image or the grid as a graph where each pixel represents a separate node of the graph and each node is 8-connected to its neighbors. Next, we apply the Breadth First Search algorithm [7] search for every node of the graph, and find all the nodes connected to the current node with same color value as the current node.

The isolation of the object does not restrict to labeling the object itself. There are semantic constraints that might need to be applied in this phase. For example, since we know that the liver cannot contain holes, any *background* area within the object needs to be relabeled as *object*.

3.4 Center detection

This phase takes as input a best-possible identification of the object in order to produce an estimation of a center around which an ACM can be initialized. Let $S \subset \Omega$ be the set of positions labeled as *object* in the Object Isolation phase. Let (x_i, y_i) be the positions in S. In order to estimate the center of the object of interest, we take into account different geometric properties of that set, giving rise to the following alternatives to find an object center $(x_c, y_c) \in \Omega$:

- *Centroid*: The center of gravity of the object is taken as the center of gravity. This strategy is problematic in scenarios with non-convex objects, since the center of gravity might in fact fall outside the object itself. The formulation to compute the centroid is:

$$x_c = \frac{\sum_{(x_i,y_i)\in S} x_i}{|S|}, \quad y_c = \frac{\sum_{(x_i,y_i)\in S} y_i}{|S|}.$$

  Note that the centroid can be interpreted as the center of mass of the object S or the arithmetic mean position of all points in S.
- *Maximum distance to the closest point to the boundary:* By analyzing the contour of the region S, we can attempt to find a center which is as far as possible from its boundary. Let $S_b \subseteq S$ be the set of pixels in the contour of S. For every $p_i \in S$, $p_i = (x_i, y_i)$ we first we compute the distance of to S_b,

$$d_{S_b}(p_i) = \min_{p_j \in S_b} m((x_i, y_i), (x_j, y_j)),$$

  for some metric m on Ω. Then, the center of the object will be the pixel that maximizes the previous expression:

$$p_c = \text{argmax}_{p_i \in S}\, d_{S_b}(p_i).$$

  Topologically, finding this center is equivalent to find the center of the largest ball contained in S, where the ball is defined by the metric m. Hence, it might be of interest in scenarios with round-like objects.

– *Minimum distance to the farthest point to the boundary*: The center expression is similar to the previous expression by changing min to max. First, we need to redefine d_{S_b} as follows:

$$d_{S_b}(p_i) = \max_{p_i \in S_b} m((x_i, y_i), (\tilde{x}_i, \tilde{y}_i)),$$

where m is again some metric on Ω, and the center will be the value that minimizes the previous expression:

$$p_c = \text{argmin}_{p_i \in S}\, d_{S_b}(p_i).$$

Topologically, finding this center is equivalent to find the center of the smallest ball that contains S, where the ball is defined by the metric m.

In terms of vector comparison, a large number of different metrics are available for point-to-point distance measurement. However, as we are modelling solid objects in $\mathbb{R}^2$, we can also consider object-related metrics, such as the geodesic distance [9].

4 Case of study

In this section, we illustrate some examples of application of our proposal to liver segmentation. Specifically, the images has been taken from a project on non-alcoholic hepatic steatosis, gathered in collaboration with the Clinica Universitaria de Navarra (Pamplona, Spain). Figure 2 shows the visually representable MRI images that we have used in the experimental results. Our goal with this case of study is to illustrate how the different alternatives in the configuration of the workflow have an impact in the final results of both the center detection procedure and the ulterior ACM.

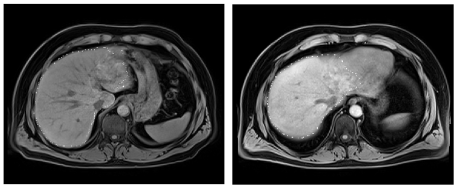

Fig. 2. Original images used in the experimental results in Section 4.

In the definition of the algorithm, we have used the proposal in Section 3. At the Object Selection phase, we have chosen 0.5 as a threshold, and the parameters in the spatial 2-fuzzy means are $m = 5$ and $p = q = 1$. At the center detection phase, we apply the following three alternatives: (a) The minimum distance to the closest point in the object using the geodesic distance; (b) the minimum distance to the farthest point using the Euclidean distance ; and (c) the centroid.

Fig. 3. In the object detection phase, the Manhattan (upper row), Euclidean (middle row), and Chebyshev (lower row) distances are used for fuzzy clustering. In the center detection phase, we have applied the maximum distance to the closest point using the geodesic distance (red), the minimum distance to the farthest point using the Euclidean distance to the second image (purple) and the centroid (blue).

Figures 3 and 4 show the results of each of the four phases of the algorithm for the images in Figure 2. Figure 3 shows the results of the image on the left and Figure 4, of the image on the right. The last column of these figures shows the center obtained using the three alternatives described above. First, we observe how the distance applied on the clustering does have an effect on the profiling of the object, although such differences are relatively erased after the object selection and object isolation phase. The center detection phase does produce severe differences on the final result of the procedure, which can be directly related to the characteristics of the metric (or centroid) used at such phase.

Overall, ee see that the best strategies for the image of Figure 3 are the centroid and the minimum distance to the farthest point using the Euclidean distance and the best strategies for the image of Figure 4 are the centroid and the maximum distance to the closest point using the geodesic distance. Therefore, from this case of study, we can state that there is no optimal strategy for all image, and the paremeterization of the workflow needs to adapted to the specific characteristics of the image or image dataset. In order to quantitatively select one parameterization for a whole dataset, a quality measure should be defined for the problem, which is currently absent from literature.

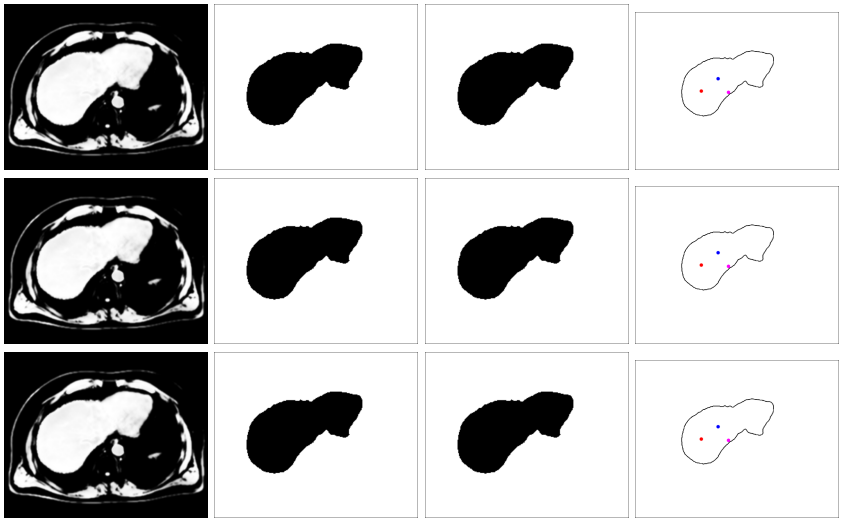

Fig. 4. In the object detection phase, the Manhattan (upper row), Euclidean (middle row), and Chebyshev (lower row) distances are used for fuzzy clustering. In the center detection phase, we have applied the maximum distance to the closest point using the geodesic distance (red), the minimum distance to the farthest point using the Euclidean distance to the second image (purple) and the centroid (blue).

5 Conclusions

In this paper we propose a strategy to find initial contours for ACMs, with the final aim of image segmentation in grayscale images. Our proposal is presented as a sequence of four phases represented as functions, so that the workflow materializes as function composition. The four phases in the strategy are:

Object detection. Usage of a spatial 2-fuzzy means algorithm to detect the membership degree of the pixels of the grayscale image.

Object selection. Transformation of the image representing the membership degree of the pixels into a binary image which contains the relevant object.

Object isolation. Application of the restrictions of the relevant object to refine the binary image obtained in the previous phase.

Center selection. Implementation of some strategies to calculate the center of the relevant object around which we will find the initial curve to apply the ACM.

As future work, we intend to extend the worflow to 3D images created as stacked MRI visualizations, so as to perform volumetric segmentations of the liver. While the mathematical tools used in our workflow are robust to dimensionality increase, the specific techniques at each phase might be adapted to cope with increasing complexity.

References

1. Bezdek, J.C., Ehrlich, R., Full, W.: FCM: The fuzzy c-means clustering algorithm. Computers & geosciences **10**(2-3), 191–203 (1984)
2. Bezdek, J., Chandrasekhar, R., Attikouzel, Y.: A geometric approach to edge detection. IEEE Trans. on Fuzzy Systems **6**(1), 52–75 (1998)
3. Bustince, H., Barrenechea, E., Pagola, M.: Relationship between restricted dissimilarity functions, restricted equivalence functions and normal EN-functions: Image thresholding invariant. Pattern Recognition Letters **29**(4), 525–536 (2008)
4. Caselles, V., Kimmel, R., Sapiro, G.: Geodesic active contours pp. 694–699 (1995)
5. Chan, T., Vese, L.: Active contours without edges. IEEE Trans. on Image Processing **10**(2), 266–277 (2001)
6. Comaniciu, D., Meer, P.: Mean shift: A robust approach toward feature space analysis. IEEE Trans. on Pattern Analysis and Machine Intelligence **24**(5), 603–619 (2002)
7. Cormen, T.H., Leiserson, C.E., Rivest, R.L., Stein, C.: Introduction to Algorithms, 3rd Edition. MIT Press (2009)
8. Crandall, M.G., Ishii, H., Lions, P.L.: Uniqueness of viscosity solutions of hamilton-jacobi equations revisited. Journal of the Mathematical Society of Japan **39**(4), 581–596 (1987)
9. Han, J., Kamber, M., Pei, J. (eds.): Data Mining: Concepts and Techniques. Morgan Kaufmann (2012)
10. Kass, M., Witkin, A., Terzopoulos, D.: Snakes: Active contour models. International Journal of Computer Vision **1**(4), 321–331 (1988)
11. Kichenassamy, S., Kumar, A., Olver, P., Tannenbaum, A., Yezzi, A.: Gradient flows and geometric active contour models pp. 810–815 (Jan 1995)
12. Li, C., Xu, C., Gui, C., Fox, M.D.: Distance regularized level set evolution and its application to image segmentation. IEEE Trans. on Image Processing **19**(12), 3243–3254 (2010)
13. Li, X., Luo, S., Li, J., et al.: Liver segmentation from ct image using fuzzy clustering and level set. Journal of signal and Information Processing **4**(03), 36 (2013)
14. Ling, H., Zhou, S.K., Zheng, Y., Georgescu, B., Suehling, M., Comaniciu, D.: Hierarchical, learning-based automatic liver segmentation. In: Proc. of the IEEE Conf. on Computer Vision and Pattern Recognition. pp. 1–8 (2008)
15. Lopez-Maestresalas, A., De Miguel, L., Lopez-Molina, C., Arazuri, S., Bustince, H., Jarén, C.: Hyperspectral imaging using notions from type-2 fuzzy sets. Soft Computing **23**(6), 1779–1793 (2019)
16. Marco-Detchart, C., Lopez-Molina, C., Fernandez, J., Bustince, H.: A gravitational approach to image smoothing. In: Advances in Fuzzy Logic and Technology 2017, pp. 468–479. Springer (2017)
17. Otsu, N.: Threshold selection method for gray-level histograms. IEEE Trans. on Systems, Man, and Cybernetics **9**(1), 62–66 (1979)
18. Perona, P., Malik, J.: Scale-space and edge detection using anisotropic diffusion. IEEE Trans. on Pattern Analysis and Machine Intelligence **12**(7), 629–639 (1990)
19. Rosin, P.L.: Unimodal thresholding. Pattern Recognition **34**(11), 2083–2096 (2001)
20. Terzopoulos, D., Witkin, A., Kass, M.: Constraints on deformable models: Recovering 3D shape and nonrigid motion. Artificial intelligence **36**(1), 91–123 (1988)
21. Weickert, J.: Anisotropic Diffusion in Image Processing. ECMI Series, Teubner-Verlag (1998)